ISSN 2395-1621

Neuro Fuzzy Based Algorithm For Thickness Computation In Trabecular Bone

[#1]T.Amutha, [#2]G.Nandhini, [#3]R.Sundaresan

[1]tamutha78@gmail.com
[2]nandhini.g22@gmail.com
[3]vit.sundaresh@gmail.com

[#12]Department of Electronics and Communication Engineering
RVSETGI,Dindigul,Tamil Nadu,India.
[#3]Assistant prof Department of Biomedical Engineering
RVSETGI,Dindigul,Tamil Nadu,India.

ABSTRACT

Adult bone diseases, especially osteoporosis, lead to increased risk of fracture associated with substantial morbidity, mortality, and financial costs. Clinically, osteoporosis is defined by low bone mineral density (BMD); however, increasing evidence suggests that the micro-architectural quality of trabecular bone (TB) is an important determinant of bone strength and fracture risk. To develop a method for processing and visualization of trabecular bone networks on the basis of magnetic resonance (MR) images acquired in the limited spatial resolution regime of in vivo imaging at which trabecular thickness is comparable to voxel size. We present a new robust algorithm and Neuro Fuzzy based new robust algorithm for computing TB thickness and marrow spacing at a low resolution achievable in vivo. The method uses a star-line tracing technique that effectively deals with partial voluming effects of in vivo imaging where voxel size is comparable to TB thickness. Error rate of the method was examined using computer-generated phantom images, while the robustness of the method is evaluated on human ankle specimens in terms of stability across a wide range of voxel sizes, repeat scan reproducibility under in vivo conditions, and correlation between thickness values computed at ex vivo and in vivo imaging resolutions. Also, the computational time of the method is examined by evaluating its ability to predict the bone strength of cadaveric specimens.Morphology is a set-theoretic approach that considers an image as the elements of a set and process images as geometrical shapes. The basic idea is to probe an image I with a simple, predefined shape, drawing conclusions on how this shape fits or misses the shapes in the image. This simple probe is called the structuring element and is a subset of the image. The typically used binary structuring elements are crosses, squares, and open disks.

Key words: trabecular bone, bone mineral density (BMD, magnetic resonance (MR)

ARTICLE INFO

Article History

Received: 27th December 2015

Received in revised form :29th December 2015

Accepted : 30th December , 2015

Published online :

31st December 2015

I. INTRODUCTION

Adult bone diseases, especially osteoporosis, lead to increased risk of fracture associated with substantial orbidity, mortality, and financial costs. Approximately, 30% of postmenopausal white women in the U.S. suffer from steoporosis and the prevalence in Europe and Asia is similar. Clinically, osteoporosis is defined by low bone mineral density (BMD) [1]. However, increasing evidence suggests that micro architectural quality of trabecular bone (TB) is an important determinant of bone strength and fracture risk. Trabecular (or spongy) bone forms a dense network of bone plates and rods and it dominates in the vertebrae and at locations near the joints of long bones (metaphysis and epiphysis). Bone atrophy as it occurs in osteoporosis leads to either homogeneous or heterogeneous thinning of the trabecular elements. Besides changes in TB network connectivity and topology, TB thickness and marrow spacing between trabeculae play critical roles in determining

the mechanical competence of bone and thus resistance to osteoporotic fractures.

The classical approach of measuring trabecular thickness is based on histomorphometry of transiliac bone biopsies. The emergence of imaging technologies such as micro-computed tomography (μ-CT) enables reconstruction of high-resolution 3-D images calling for more elaborate techniques for computing TB thickness. Recently, in vivo imaging techniques including magnetic resonance imaging (MRI) , high-resolution peripheral quantitative CT (HR-pQCT), and multirow detector CT (MD-CT) have emerged as promising modalities for high-quality TB imaging at peripheral sites that avoid the problems of invasive bone biopsies. Therefore, an accurate and robust algorithm for computing TB thickness and marrow spacing that is applicable to in vivo imaging would be useful as an effective indicator of quantitative bone quality for clinical trials designed to evaluate fracture risks under different clinical conditions. Here, we present such an algorithm and evaluate its accuracy, robustness, and sensitivity to bone strength. Although in this paper, the method is applied and evaluated on MD-CT imaging.

Here, we introduce a star-line-based algorithm for an accurate and robust measure of TB thickness and marrow spacing at in vivo resolution in the presence of significant partial voluming. Accuracy of the method was examined on computer-generated phantoms. Robustness of the method was evaluated on human specimens in terms of stability across a wide range of voxel sizes, repeat scan reproducibility under in vivo conditions, and correlation between thickness values computed at ex vivo and in vivo imaging resolutions. Also, the sensitivity of the method was examined by its ability to predict bone strength of cadaveric specimens. Finally, the method was evaluated in a sample of young adult volunteers with tibial scans.

The modern techniques of artificial intelligence have found application in almost all the fields of the human knowledge. However, a great emphasis is given to the accurate sciences areas, perhaps the biggest expression of the success of these techniques is in engineering field. These two techniques neural networks and fuzzy logic are many times applied together for solving engineering problems where the classic techniques do not supply an easy and accurate solution. The neuro-fuzzy term was born by the fusing of these two techniques. As each researcher combines these two tools in different way, then, some confusion was created on the exact meaning of this term. Still there is no absolute consensus but in general, the neuro-fuzzy term means a type of system characterized for a similar structure of a fuzzy controller where the fuzzy sets and rules are adjusted using neural networks tuning techniques in an iterative way with data vectors (input and output system data).

II. EXISTING METHOD

Theory and algorithms

The new method for thickness computation of the fuzzy digital objects interprets fuzzy membership value at a given image voxel as the partial occupancy of the object or the local object material density. Although, the method is designed for fuzzy digital objects at low resolution, its premise is built on objects in the continuous space. First, we establish a definition of “local thickness” in the continuous space, and then, we describe an effective algorithm for digital objects.

BLOCK DIAGRAM Local Thickness

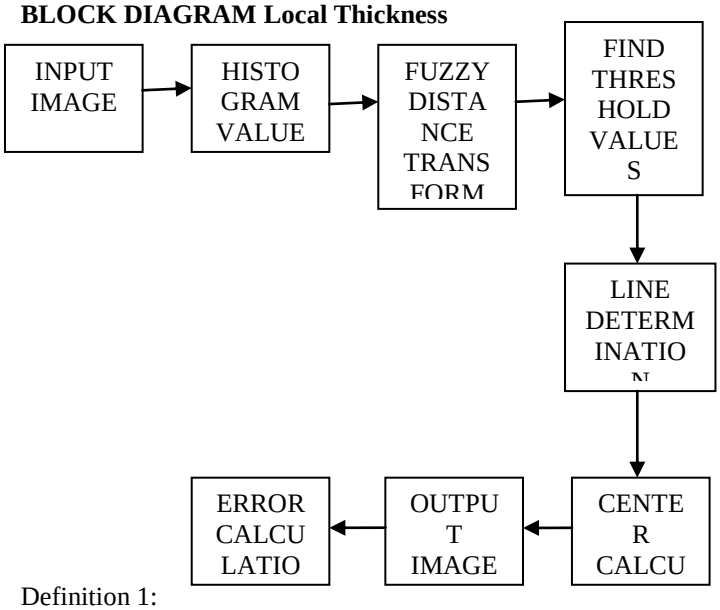

Definition 1:

For any object O ⊂ R3 and any point p ∈ O, the thickness of O at p, denoted as τO (p), is the length of the diameter of the MIB inMO (p), whose circumference is farthest from p. It can be shown that, for any object O ⊂ R3 and a point p ∈ O, the MIB in MO (p) whose circumference is farthest is unique. Therefore, Definition 1 produces a unique thickness distribution for any object.

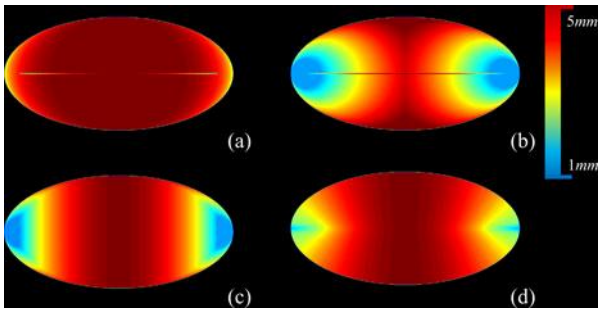

Fig. 1. Comparison among different definitions of thickness in terms of satis- fying Property 1. The color bar is added where the thickness values are shown in millimeter units. (a) Local thickness distribution on an ellipse.

Thickness Computation for Fuzzy Digital Objects

The proposed thickness computation algorithm for fuzzy digital objects is summarized in three steps:

Step 1: Computation of the surface skeleton A of a fuzzy digital object O.

Step 2: Computation of thickness τO(a) at all the axial voxels a ∈ A.

Step 3: Inheritance of thickness τO(p) at all the nonskeletal voxels p ∈ O − A following Definition 1.

Here, an intercept-based algorithm is introduced for computing thickness at axial voxels that overcomes the digitization error. Let us consider a voxel p ∈ O in a fuzzy object O; an intercept of O at p along a direction (polar: θ, azimuth: φ) is the membership-weighted length of the straight line segment lθ,φ(p,O) passing through p with the two ends coinciding with the boundary of O. It should be noted that, for a voxel p ∈ O, there can be many intercepts of O passing through p. Let_O (p) denote the set of all

possible intercepts of O that pass through p. The thickness measure τO(a) at an axial voxel a is approximately equal to the length of the shortest intercept of O passing through a.

Major advantages of this approach are that 1) the minimum-intercept length measure is highly robust under small random shifts of axial voxels, and 2) partial voluming effects are efficiently handled during intercept length computation. Here, we analytically discuss the relevance of the digitization error in the FDT-based and the new thickness computation methods.

The FDT-based approach assumes that an axial voxel where the FDT value is sampled coincides with the true axis of the object and any difference between the two directly contributes to thickness error. In case of the intercept-based approach, the true axis of an object always orthogonally intersects a minimum intercept line. Therefore, even when an axial voxel deviates from the true axis, the error caused by the intercept approach is minimized.

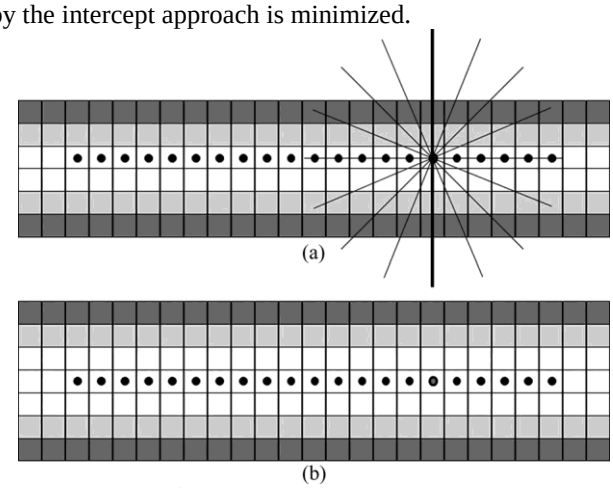

Fig. Advantages of intercept-based thickness computation in reducing digitization errors as compared to the FDT-based method.

The star-line-based thickness computation algorithm (see Fig. 4) determines the term minl∈_O(a) π(l) at axial voxels. It locally traces an object alongmpairs of mutually opposite sample lines emanating from an axial voxel a (black dot in Fig. 4). These sample lines are selected at a pseudouniform distribution over the entire 3-D angular space. A parameter ψ is used to define the angular separation between neighboring sample lines. The optimum value of ψ was experimentally determined and used for all experiments.

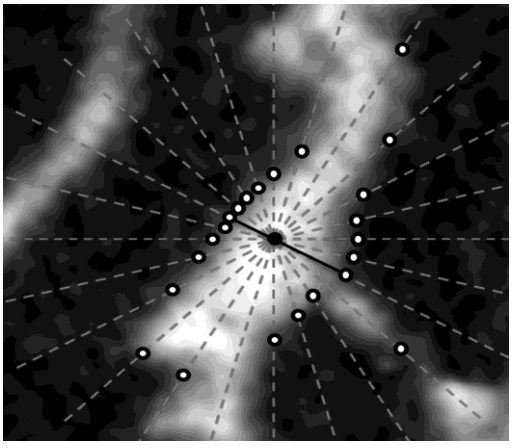

Fig. 4. Illustration of star-line-based TB thickness computation in two- dimensions. The candidate voxel (black dot), star-lines (dot), edge locations (hollow dots), and shortest intercept (solid line) in TB thickness computation are shown.

III. EXPERIMENTAL METHODS

The experimental study was designed to evaluate the following performance indices: 1) accuracy; 2) stability of local thickness values under random local shifts in axial voxels; 3) stability of local thickness values across a wide range of image voxel sizes; 4) stability of thickness values under a major shift in "true" image resolution using ex vivo and in vivo imaging modalities; 5) repeat scan reproducibility; 6) ability of TB thickness and marrow spacing to predict bone strength; and 7) application to in vivo studies.

The following sequence of steps was applied to each specimen: 1) MD-CT imaging; 2) removal of soft tissue and dislodgement of the distal tibia from the ankle joint; 3) μ-CT imaging; 4) specimen preparation and TB core extraction; and 5) mechanical testing to compute compressive Young's modulus and yield stress. Assuming that the thickness computation using μ-CT at high resolution is quite accurate, this experiment examined the meaningfulness of thickness computation using the current method and an in vivo imaging technique. In the rest of this paper, voxel size or digitization will refer to down sampling effects while resolution will symbolize the effects of the MTF on an imaging technique.

Bone Volume Fraction and Volume Fraction Image Computation

To compute trabecular thickness, a fuzzy representation of TB is used where the membership value at a given p represents its bone volume fraction (BVF) denoted as BVF(p).

For μ-CT images, BVF was directly computed from the raw CT data using the bimodal intensity distribution. MD-CT imaging acquires data in Hounsfield units and these numbers were first converted to BMD (mg/cc) measures using a calibration phantom.

Marrow space represents the marrow-filled region between trabeculae. Therefore, marrow spacing was computed from the marrow volume fraction image (MVF), derived as the inverse of the BVF image as follows:

$$MVF(p) = 1.0 - BVF(p).$$

Both BVF and MVF images were resampled using the windowed-sinc interpolation method producing 0.15-mm isotropic voxels.

TB Thickness and Marrow Spacing Measures

Computation of both trabecular thickness and marrow spacing was accomplished using the algorithm described in Section II-B. Specifically, the two TB measures, namely, TB thickness (TH_B) and marrow spacing (SP_M), were computed over a target volume-of-interest (VOI) V as follows:

$$TH_B = TH_B(p)/|V_B|$$
$$SP_M = SP_M(p)/|V_M|$$

where V_B (or V_M) is the set of voxels with nonzero BVF (respectively, MVF) in V. In addition to THB and SPM, the average BMD over V was computed.

Optimum Angular Separation Parameter

As described in Section, the value of the parameter ψ defining the angular separation between neighboring sample lines needs to be determined. A small value of ψ provides a more precise measure of star-line-based thickness at higher computation cost and the right choice of the

parameter depends on the tradeoff. To understand the tradeoff between accuracy and computation cost, an experiment was conducted on in vivo MD-CT images of the distal tibia from ten human volunteers. The ideal measure of star-line-based local thickness distribution was determined at dense distribution of star-lines with $\psi = 1^{\circ}$.
At any other value of ψ, the mean and standard deviation of voxel wise thickness errors were computed. The mean error was expressed as a percentage of the ideal mean thickness measure (see Fig. 5). Also, the computation time was expressed as a percentage of time required at one degree angular separation (see Fig. 5). An overall tradeoff measure was defined as the square root of the sum of squares of normalized error and computation time.

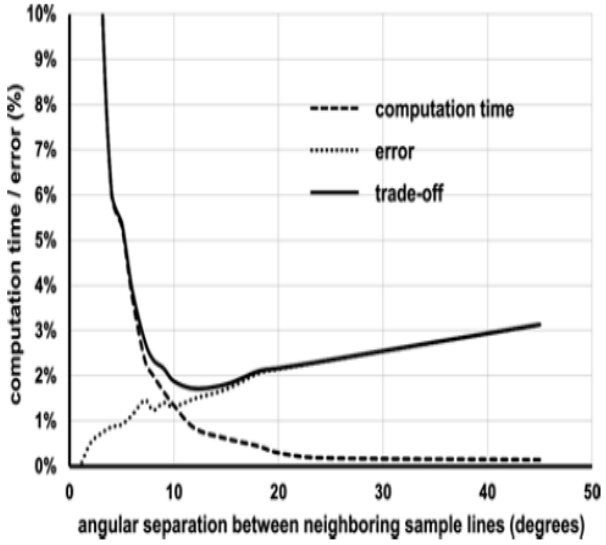

Fig. 5. Tradeoff between computation time and error as a function of the parameter ψ defining the angular separation between neighboring sample lines for star-line-based computation of local thickness.

VOI Selection for Cadaveric Image Analysis

The size and location of VOIs for image analysis of the ca- daveric bone strength study (Experiment 6) were chosen as per the information recorded during specimen preparation for me- chanical testing of individual specimens. First, the image was rotated to align the bone axis along the coordinate z-axis using the following two steps: 1) generation of a cylinder C with its axis lying on the coordinate z-axis and its cross-sectional area equating to the average tibial cross sectional area; and 2) reorientation of the tibial volume to align its axis with C by maximizing the overlap between the tibial volume and the cylinder C.

After reorienting the bone image, a VOI cylinder of 8-mm diameter along the coordinate z-axis was generated and its proximal end was manually positioned at the center of the cortical rim us- ing in-plane translation through a graphical user interface. The location of the distal end of the VOI cylinder in the slice direction and its length were determined as per the core location and length recorded during specimen preparation; the growth plate was visually located in the CT data of each specimen. Finally, the central 6-mm region from the cylinder was used as the VOI for the extensometer test; for the non-extensometer study, the length of the VOI was determined as per data collected during specimen preparation for the second mechanical test.

Discussion and results of existing method

Results of TB thickness measures for three specimens with different bone strengths are illustrated in Fig. 7. As observed in the figure, an 8% difference in BMD from a strong bone (a) to a weak bone (c) leads to a 70% loss in bone strength and manifests as a 20% reduction in TB thickness and a 42% increase in marrow spacing. This observation supports that TB thickness and marrow spacing measures are highly sensitive to bone loss and, therefore, play a significant role in early detection of bone diseases.

IV. PERFORMANCE

- ✓ Accuracy Analyses
- ✓ Robustness Under Different Conditions
- ✓ Reproducibility Analysis
- ✓ Ability to Predict Bone Strength

Reproducibility Analysis

Three repeat MD-CT scans of 15 cadaveric ankle specimens were used to examine the method's reproducibility. Fig. 12 illustrates a color-coded TB thickness map over a matching volume in two repeat MD-CT scans of the distal tibia. For quantitative analyses, ten spherical VOIs of the same radius were randomly selected in the first MD-CT scan of each specimen above the position 8-mm proximal to the distal endplate leading to a total of 150 VOIs. A post registration algorithm was used to locate the matching VOIs in the second and third repeat scans. It is obvious that the result of reproducibility analysis depends on the scale of the VOI, with larger VOIs showing improved reproducibility. The relationship between the method's reproducibility and VOI size is presented in Fig. 13.

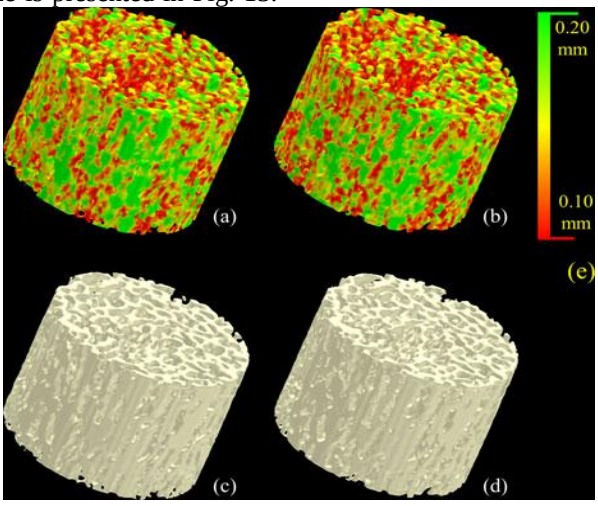

Fig. 12. Illustration of reproducibility of the TB thickness measure under MD-CT repeat scans. (a) and (b) Color-coded TB thickness images. (c) and (d) TB image without color coding. (e) Color coding bar.

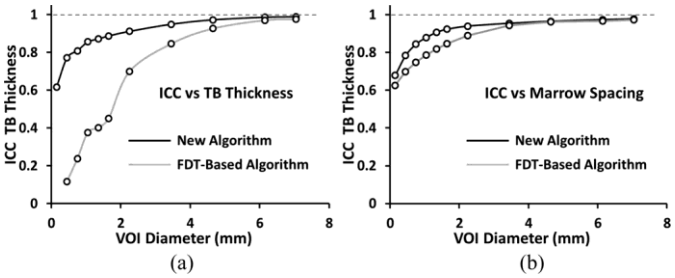

Fig. 13. Illustration of repeat MD-CT scan ICC values as a function of VOI diameters for both the new and the FDT-based algorithms. As observed in (a), at a VOI diameter of 3.45 mm or greater, the ICC value for the new algorithm exceeds the mark of 0.95, while the FDT-based algorithm requires a VOI diameter of 6.15 mm.

Robustness Under Different Conditions

The linear correlations of TB thickness and marrow spacing com- puted from registered μ-CT and MD-CT images are presented in Fig. 11. The r values from a linear regression model of TB thickness and marrow spacing measures in two different modal- ities are 0.96 and 0.95, respectively, with slopes of 1.66 and 1.08, respectively. For both measures, the regression line passes near the origin.

Thus, the results of this experiment reveal that the thickness values computed by the current method from two distinctly different modalities are not identical, but there is a strong association between their values.

Ability to Predict Bone Strength

The results of correlation analysis between Yield stress and each of the TB thickness and marrow spacing measures using the new method are shown in Fig. 14(a) and (b), while the results using the FDT-based algorithm are shown in Fig. 14(c) and (d).

The values of R^2 or coefficients of determination from the linear regression analysis between TB Young's modulus and the different TB measures are presented in Table II. For both yield stress and Young's modulus parameters, the TB thickness and mar- row spacing measures computed using the new method have demonstrated superiority in predicting bone strength as com- pared to the FDT-based measures and MD-CT based volumetric BMD.

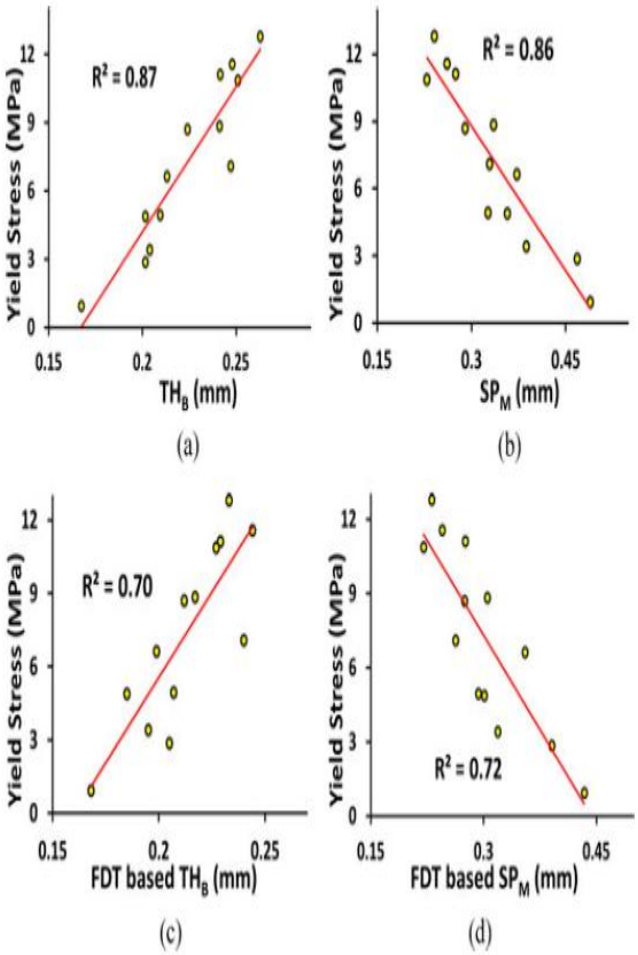

Fig. 14. (a) and (b) Ability of TB thickness and marrow spacing measures computed by the method to predict experimental bone strength. The ability is computed in terms of the R^2 of linear correlation between bone strength and the respective measure. (c) and (d) Same as (a) and (b) but for the FDT-based method.

Results of In Vivo Pilot Studies

Twenty male and twenty female volunteers (19 to 21 years) were used to form body mass index (BMI) order-matched male–female pairs. The BMI was 26.89 ± 6.32 kg/m^2 (mean±standard deviation) for males and 25.15 ± 7.96 kg/m^2 for females, and r for the two ordered groups of BMIs was 0.98.

The colored results for one male–female pair are shown in Fig. 15. Clearly, the results indicate that the male has thicker TB than the female. Quantitative results show that males on average have 6.7% thicker TB and 13.9% reduced marrow spac- ing as compared to females. Observed values for TB thickness and marrow spacing for males were 0.22 ± 0.02 and 0.32 ± 0.06

Disadvantages

- Incapable to generalize the method, depends only on rules
- Not robust in relation the topological changes of the system.
- Depends on the existence of a expert to determine the inference logical rules

V. PROPOSED METHOD

A neuro-fuzzy system can be interpreted as a set of fuzzy rules. This system can be total created from input output data or initialised with the à priori knowledge in the same way of fuzzy rules. The resultant system by fusing fuzzy systems and neural networks has as advantages of learning through patterns and the easy interpretation of its functionality.

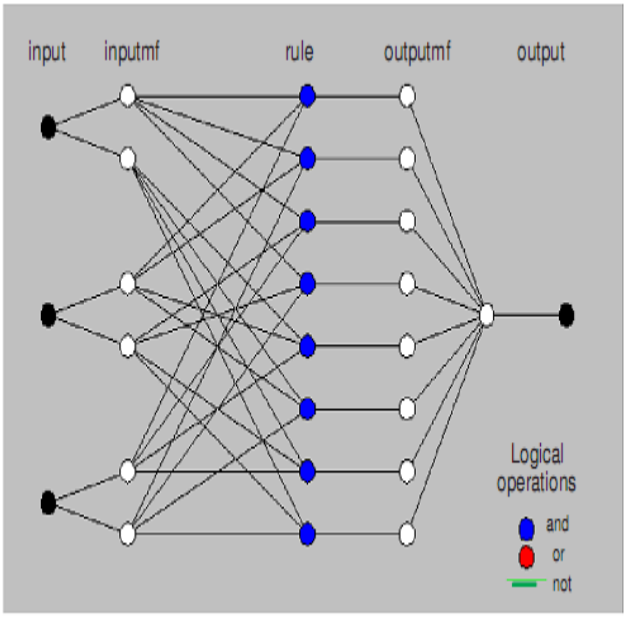

The structure of the obtained neural network.
There are several different ways to develop hybrid neuro-fuzzy systems, therefore, being a recent research subject, each researcher has defined its own particular models. These models are similar in its essence, but they present basic differences.

Many types of neuro-fuzzy systems are represented by neural networks that implement logical functions. This is not necessary for the application of an learning algorithm in to a fuzzy system, however, the representation trough a neural networks is more convenient because it allows to visualise the flow of data through the system and the error signals that are used to update its parameters. The aditional benefit is to allow the comparison of the different models and visualise its structural differences. There are several neuro-fuzzy architectures_like:

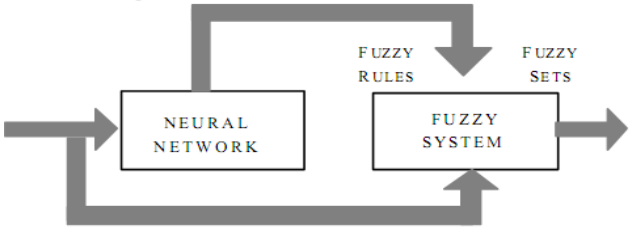

Figure 1. Cooperative Systems

VI. METHODOLOGY

The methodology of this work entails the use of a neuro-fuzzy system, which is a software program utilizing the benefits offered by the Matlab toolboxes. The only re- quirement of this system is the availability of a training set that allows for a fuzzy rule base that is capable of clas- sifying the pixels after the neural network training.

This training set is constructed using training images shown in Fig. 1. These images are distinct combinations of the three classes of regions described above. The output data of the training set, depicted in Fig. 3, are images created to model the ideal output (three classes) of the classifying algorithm. The training data are used to generate fuzzy inference systems (FIS) for each of the three classes.

Problems encountered in the field of image processing frequently reside in the vagueness of the data under study. Over the last few decades neural networks and fuzzy systems have established reputation as an alternative approach to information processing. Both have certain ad- vantages over classical methods, especially when vague data or prior knowledge is involved. However, their applicability suffers from several weaknesses of the individual methods.

A neuro-fuzzy approach as a combination of neural networks and fuzzy logic has been introduced to overcome the individual weaknesses and to offer more appealing features. The ultimate goal of applying such a system is to get rid of imprecise information present in an image such as pixel grayness ambiguity, geometrical segmentation of the image and the uncertain interpretation of a scene [2].

This exploits, respectively, the learning capabilities and the descriptive power of systems, thus providing results characterized by a high interpretability and good degree of accuracy [1, 2].

An image feature is what distinguishes and character- izes it from other images [3, 4, 5]. The aim of the neuro- fuzzy approach application is to extract these features pixel by pixel and classify them into three sets of classes: Regular, Texture and Contour.

The concept of the edge is greatly connected with feature extraction methods [7, 8].

The difficulty of such a system lies in detecting tex- tures the presence of which dictates the use of multi-scale representation. The method proceeds without any prior knowledge or presence of any expert intervention and can be employed as a pre-processing or a post-processing stage of an image segmentation problem. It may be also used to improve the performance of some database re- trieving processes [6]. Furthermore, it can be applied in biomedical context especially in human body images for purposes of analytical studies. It would ultimately lead to a system that would help after applying appropriate en- hancement techniques to recognize abnormalities in the biomedical images and thus help the physician in his/her diagnostic procedures.

This paper aims at implementing the above-mentioned approach in image pixel classification. The

objective is to use such an approach in developing a functioning program that will accept any input image and classify its pixels one by one into the three distinct classes indicated above.

The Neuro-Fuzzy approach presented here allows any ordinary person without experience in this field and with the availability of only a training set with ideal outputs to build up a system that models his/her information with no more than two or three functions based on well- known and well-established algorithms. The technique would then use the classification to localize regions that may be used to detect any abnormalities and list the diagnosis accordingly. The application can be easily used as a pre-processing technique, where classified images can be used in a number of applications of analytical nature. Computer analysis can complement to laboratory tests for example, that might give a clearer picture of the human physiology and pathological diseases.

Biomedical imaging modalities, such as MRI and CT-scans showed high accuracy in all three classes of pixels. These results were very encouraging since these images are of great importance in the diagnosis of hard-to-detect diseases. These kinds of images have great contrast values for edges and clearer regions that allowed this approach to easily react to such images. The proposed system was insensitive to the noise imposed in these images, thus, maintaining its levels of high accuracy.

The system ability in solving the texture classification that might be extremely hard or even impossible in other methods is the main contribution of this work. Its regular class is also highly accurate, and very close to a human observer's classification. The proposed technique is a highly useful and powerful classification tool that fulfilled the independency requirement of being a self automated classification tool.

VII.CONCLUSION

In this paper, we presented a new thickness computation algorithm for fuzzy digital objects at relatively low resolution and investigated its role in computing TB thickness and marrow spacing measures in vivo conditions. It was proved that neuro-fuzzy approach could be one of the important modalities in image processing, especially in the biomedical scene where most diagnostic techniques rely on imaging. The presented pixel classification tool is a highly useful, powerful, and independent of any expert or any prior knowledge. The effectiveness of this method and its ability to automatically extract the shape and texture properties from an image drive us to consider it a highly intelligent development in image processing that supports intelligent decision at low costs. The suggested approach may be enhanced by some pre-processing procedures that might boost the characteristics of the system in its classification. Some adjustments in the learning schemes or the training sets can also increase the efficiency of the system, especially choosing the optimal subtractive clustering parameters. This encourages us to subject it to future improvement and enhancement that will enrich its contribution and find ways for its real imaging applications. This method uses a star-line tracing technique that effectively deals with partial voluming effects of in vivo imaging where voxel size is comparable to TB thickness. We estimated that our Neuro Fuzzy method is better than Fuzzy approach in terms of error calculation and computation time.

REFERENCES

[1] G. Diederichs, T. M. Link, M. Kentenich, K. Schwieger, M. B. Huber, A. J. Burghardt, S. Majumdar, P. Rogalla, and A. S. Issever, "Assessment of trabecular bone structure of the calcaneus using multi-detector CT: Correlation with microCT and biomechanical testing," Bone, vol. 44, pp. 976–983, 2009.

[2] P. K. Saha, Y. Xu, H. Duan, A. Heiner, and G. Liang, "Volumetric topo- logical analysis: a novel approach for trabecular bone classification on the continuum between plates and rods," IEEE Trans. Med. Imag., vol. 29, pp. 1821–1838, Nov. 2010.

[3] Y. Xu, G. Liang, G. Hu, Y. Yang, J. Geng, and P. K. Saha, "Quantification of coronary arterial stenoses in CTA using fuzzy distance transform," Comput. Med. Imag. Graph, vol. 36, pp. 11–24, 2012.

[4] P. K. Saha, Z. Gao, S. K. Alford, M. Sonka, and E. A. Hoffman, "Topo- morphologic separation of fused iso-intensity objects via multi-scale open- ing: separating arteries and veins in 3-D pulmonary CT," IEEE Trans. Med. Imag., vol. 29, no. 3, pp. 840–851, Mar. 2010.

[5] P. K. Saha and F. W. Wehrli, "Measurement of trabecular bone thickness in the limited resolution regime of in vivo MRI by fuzzy distance transform," IEEE Trans. Med. Imag., vol. 23, no. 1, pp. 53–62, Jan. 2004.

.

[6] R. Moreno, M. Borga, and Ö. Smedby, "Estimation of trabecular thickness in gray-scale images through granulometric analysis," Proc. SPIE, 2012, pp. 831451-1–831451-9, 2012, to be published.

[7] Y. Liu, D. Jin, and P. K. Saha, "A new algorithm for trabecular bone thickness computation at low resolution achieved under in vivo condition," in Proc. 10th Int. Symp. Biomed. Imag., San Francisco, CA, USA, 2013, pp. 390–393.

[8] Y. Liu, P. K. Saha, and Z. Xu, "Quantitative characterization of trabecular bone micro-architecture using tensor scale and multi-detector CT imag- ing," in Proc. Image Comput. Comput.-Assisted Intervention Conf., Nice, France, 2012, pp. 124–131.

[9] G. Borgefors, "On digital distance transformation in three dimensions," Comput. Vis. Imag. Understanding, vol. 64, pp. 368–376, 1996.

[10] C. Arcelli, G Sanniti di Baja, and L. Serino, "Distance-driven Skeletoniza- tion in voxel images," IEEE Trans. Pattern Anal. Mach. Intell., vol. 33, no. 4, pp. 709–720, Apr. 2011.

